

TM 659

TECHNICAL MEMORANDUMS

NATIONAL ADVISORY COMMITTEE FOR AERONAUTICS

NACA-TM

No. 659

DISINTEGRATION OF A LIQUID JET

By A. Haenlein

Forschung auf dem Gebiete des Ingenieurwesens
Vol. II, No. 4, April, 1931

REPRODUCED BY
NATIONAL TECHNICAL
INFORMATION SERVICE
U. S. DEPARTMENT OF COMMERCE
SPRINGFIELD, VA. 22161

Washington
February, 1932

TECHNICAL MEMORANDUMS
NATIONAL ADVISORY COMMITTEE FOR AERONAUTICS

No. 659

DISINTEGRATION OF A LIQUID JET

By A. Haenlein

Forschung auf dem Gebiete des Ingenieurwesens
Vol. II, No. 4, April, 1931

Washington
February, 1932

NATIONAL ADVISORY COMMITTEE FOR AERONAUTICS

TECHNICAL MEMORANDUM NO. 659

DISINTEGRATION OF A LIQUID JET*

By A. Haenlein

I. THE PROBLEM

In the compressorless Diesel engine the fuel is injected under high pressure through one or more fine nozzles (0.1 to 1.0 mm diameter) directly into the combustion space or into an antechamber. For a knowledge of the processes which take place in the combustion space, it is important to know how the injected fuel is atomized and how it is mixed with the surrounding air. This question has been the subject of a series of researches. The effect of the injection pressure, jet velocity and physical properties of the liquid on the size of the drops and on their penetrating ability has been investigated partly by theory and partly by experiment. (Reference 1.)

In this work I set myself the task of determining experimentally the process of disintegration and atomization in its simplest form, and of thus investigating the influence of the physical properties of the liquid to be atomized on the disintegration of the jet. Particular attention was paid to the investigation of the process of atomization. The experiments were performed in the engine laboratory of the Dresden Technische Hochschule at the suggestion of Doctor A. Nagel, whom I take this opportunity of thanking. I am also under particular obligation to Doctor C. Weber, who stood tirelessly at my side during the performance and evaluation of the experiments. The apparatus was purchased with funds supplied by the Notgemeinschaft der Deutschen Wissenschaft, for which I hereby express my thanks.

*"Ueber den Zerfall eines Flüssigkeitsstrahles." Forschung auf dem Gebiete des Ingenieurwesens, April, 1931, pp. 139-149. Accepted as a dissertation by the Dresden Technische Hochschule (Institute of Technology).

In order to simplify the work of observation as much as possible, the study of a jet in compressed air, as well as of one subjected to periodic impulses, was avoided, and the investigation was limited to a jet flowing uninterruptedly into a free space up to velocities of 70 m/s. The work is a contribution toward the solution of the problem of jet disintegration. Further researches on this subject are now in progress at the Dresden Technische Hochschule.

II. THE LIQUIDS TESTED

In the choice of the liquids for investigation, it was endeavored to obtain wide differences in their physical properties. This was possible, however, to only a limited degree, since the liquids coming under consideration showed notable differences only in their viscosity (greatest difference 1:880), while their surface tension and density varied only in the ratio of 1:2.1 and 1:1.4, respectively. The liquids chosen for investigation were water, gas oil, glycerine and castor oil. Their physical constants and the method for determining them are given in Table I.

TABLE I. Physical Constants of Liquids Tested

Determined by		Water	Gas oil	Glycerine	Castor oil	Dimension
Hydrometry	Sp. gr. γ	1.0	0.86	1.23	0.96	g/cm^3
	density $10^3 \rho$	1.02	0.876	1.25	0.98	$g \cdot s^2/cm^4$
Engler apparatus at 20°C	Viscosity $10^5 \eta$	10.2	83	930	8600	$g \cdot s/cm^2$
	$\nu = \eta/\rho$	0.010	0.0955	0.745	8.78	cm^2/s
Capillary method	Surface tension α	0.072	0.035	0.066	0.034	g/cm
	α/ρ	70.8	40.0	52.7	34.7	cm^3/s^2
Drop method	Surface tension α	0.072	0.036	0.066	0.035	g/cm
	α/ρ	70.8	41.1	52.7	35.7	cm^3/s^2

III. THE APPARATUS

a) Arrangement for nozzles of 0.1 to 0.2 mm diameter.— With small nozzle bores (0.1 to 0.2 mm diameter), pressures of 300 to 400 atmospheres were necessary for the jet to attain sufficient velocity. To obtain these pressures, the fuel pump of a Junkers Diesel engine was used, which supplied 0.47 cm³ per stroke at $n = 400$ r.p.m.

Figure 1 is a diagram of the apparatus. From the container the test liquid flows to the pump through filter I. The pump is actuated by a cam and forces the liquid through the nozzle from which the jet flows. Two pressure gauges, for ranges of 0 to 120 atmospheres and 0 to 2000 atmospheres, were connected with the pressure tube in front of filter III. The usual fine gauze filters I and II were not sufficient for nozzle bores of 0.1 to 0.3 mm. Hence there was introduced, just before the nozzle, a special filter, which was filled with glass beads of 0.2 to 0.3 mm diameter and produced the requisite degree of purification. In order to diminish the pressure variations due to the separate pump strokes, an accumulator I was connected with the pressure tube. For this purpose a coil of seamless steel tubing of 9 mm inside and 25 mm outside diameter was used. The total length of the tube was 30 m and its capacity was 1900 cm³.

The flow was regulated as follows:

1. By regulating the frequency of the pump strokes.
(The speed of the pump motor could be controlled within a range of 200 to 400 r.p.m..)
2. By varying the amount passing through an overflow valve.

b) Arrangement for nozzles of 0.3 to 0.5 mm diameter.— The output of the pump was not sufficient to produce the desired exit velocity for nozzles of more than 0.3 mm diameter. The necessary pressure was therefore produced as follows. (Fig. 1.) The accumulator I was connected with a pressure chamber 2, which could be charged to about 100 atmospheres by means of a compressed-air cylinder. Simultaneously the nozzle was closed by an easily removable needle valve. The pump then acted through the accumulators I and II and gradually compressed the air

cushion in the accumulator II. When the pressure attained the desired value, the needle valve was removed and the liquid flowed out under gradual pressure decrease. Thus it was possible to keep the pressure and velocity approximately constant during the course of an experiment lasting about five seconds. By means of this arrangement, pressures up to 600 atmospheres could be obtained and nozzles up to 0.5 mm diameter could be tested. With larger diameters the sudden pressure drop on opening the nozzle was so great that observation of the jet was impossible.

c) Arrangement for nozzles of 0.7 to 2.0 mm diameter.- The following arrangement (fig. 2) was used to investigate these diameters. A cylindrical steel vessel of 18,000 cm³ capacity for pressures up to 200 atmospheres had its bottom connected with the nozzle and its top with a compressed-air cylinder. This vessel was about two-thirds filled by means of a pipe with the liquid under investigation and was then subjected to the pressure of the compressed air. The pressure in the vessel could be kept approximately constant for the duration of the flow by the proper adjustment of the valve on the air cylinder. To be on the safe side, this arrangement was used only for pressures up to 120 atmospheres.

d) The nozzles.- These were supported by a nozzle holder fastened to a heavy iron plate, which was separated from the rest of the apparatus in order to keep it as free as possible from vibrations. The nozzle was secured by a nut to the nozzle holder, which was ground flat on its front side. No further packing was necessary at this point. To facilitate observation of the orifice, the nozzle plate was made to project somewhat from the bore of the nut. After leaving the nozzle, the jet developed freely and horizontally in space for about 6 meters and then struck a receiving screen, which conducted the liquid into a vessel.

The nozzles were made of brass, in order to facilitate working. They were bored by steel drills. The ratio of diameter to length of bore was 1:10 for all the nozzles. The inlet and exit orifices were not rounded. They were measured under the microscope by means of an ocular micrometer. The diameters were measured for every 45° and the mean taken. Since, with the exceptionally slender steel drills which had to be used to make the

holes and a vibration of the drills was probable, it was possible for inlet and exit orifices to be considerably widened. Therefore the narrowest part of the bore was determined by a capillary measurement. The nozzle was clamped by means of a nut to the smoothly ground surface of a small glass tube. The end of this tube dipped into a liquid of known surface tension. The surface of this liquid was then lowered until the thread of liquid broke off in the nozzle. This moment was determined by means of a microscope. The diameter of the nozzle was then determined from the measured rise. The measured diameters are given in Table II. For comparison, tests were made with a glass tube of 1 mm diameter, which yielded the same results as the 1.04 mm brass nozzle.

TABLE II. Nozzle Diameters

Nozzle number	Nozzle length mm	Optically measured at		Measured by capillary method mm	Mean value mm
		inlet mm	exit mm		
1	1	0.12	0.12	0.11	0.12
2	2	0.21	0.23	0.22	0.22
3	3	0.31	0.32	0.31	0.31
4	5	0.52	0.50	0.50	0.51
5	7	0.71	0.71	0.70	0.71
6	10	1.03	1.05	1.03	1.04

e) Method of observing the jet.— The observation of the jet with the naked eye was insufficient at the velocities investigated (up to about 100 m/s). Therefore instantaneous photography was resorted to. The illumination time necessary to obtain sharp pictures could be estimated from the order of magnitude of the drops and of the jet velocity.

If the mean drop diameter is estimated at about 0.1 mm, a drop at a velocity of 100 m/s will move about 1 mm, or ten times its diameter, in 10^{-5} seconds, so that it will appear as a streak on the photographic plate. The illumination time must therefore be considerably less than 10^{-5} seconds. To attain such a brief illumination, use was made of electric sparks, which are often employed for the observation of high velocities.

For jets of not less than 0.2 mm diameter, simple shadow pictures sufficed. From the light source shown in Figure 3, a shadow picture of the jet was cast on a highly sensitized silver-bromide paper stretched on a board about 90 cm long and protected from the spray by a glass plate. The distance from the light source to the jet was about 70 cm; that from the jet to the paper, 5 to 7 cm. Because of the great length of the picture, the spherical drops appear as ellipses at the ends of the picture. The sharpness of the edges of the picture was diminished by the fact that the spark gap was not a punctiform source of light. For a jet diameter of 0.1 mm, a microscopic camera was used, but no further pictures were taken with this camera after it was found that the same typical phenomena occurred.

To obtain the spark, the following arrangement, shown in Figure 4, was used. An influence machine charged the condenser I, which consisted of a battery of two Leyden jars. The circuit I could be closed through the series spark gap F_1 by a switch, thus charging the condenser II, which was also connected with the circuit II. In this circuit was the illuminating spark gap F_2 . The length of the spark gap F_1 was about 20 mm, and that of the spark gap F_2 about 11 mm, so that the circuit I was considerably more damped. The illumination period could be approximately estimated from the dimensions of the conductors and condenser.

With sufficient damping it may be assumed that only the first half oscillation of the spark makes a perceptible impression on the photographic paper. This half oscillation requires the time

$$t = \pi \sqrt{CL},$$

where C is the capacity and L is the self-induction. For the circuit II, the capacity C was 6×10^{-19} s²/cm, and L was 3700 cm. Therefore the time t was about 1.5×10^{-7} s, which corresponded to the illumination time required.

The jet velocity was determined by measurement of the liquid flowing from the nozzle, by means of a stop watch and a measuring glass. The length of each determination was 5 to 20 seconds.

IV. CHARACTERISTIC DISINTEGRATION PHENOMENA

a) Surface disturbances.— By means of the arrangement described, about 200 pictures were taken, several of which, typical for different liquids, are reproduced in Figures 10 to 13.

Out of all the pictures a series of characteristic jet forms can be found. These appear more or less clearly defined for each liquid and for each jet diameter under certain definite conditions. The jet is not perfectly cylindrical on leaving the nozzle. Its surface is subject to slight disturbances which are due to various conditions, such as vibrations of the nozzle, imperfect roundness of the orifice, vibrations of the whole apparatus, particles of dust or air bubbles in the jet, vortex formation in the nozzle and the influence of the surrounding air. The most important are rotationally symmetric disturbances, as in Figures 5a and 5b, and one-sided wave-like disturbances, as in Figure 5c, which occur in different planes. The ratio of the wave length to the jet diameter (l/d) is characteristic of its effect on the jet. The initial disturbances occur simultaneously and overlap one another. These disturbances increase or decrease, according to the forces acting on them and thus lead to the disintegration of the jet.

b) Drop formation without the influence of the air.— At low velocities the air does not appreciably affect the shape of the jet. The only disturbing force then acting on the jet is the surface tension. Under its influence the liquid cylinder becomes an unstable body which, under certain rotationally symmetric disturbances of its cylindrical shape, breaks up into separate drops. This phenomenon has already been investigated by Lord Rayleigh for nonviscous liquids. (Reference 2.) He found that the drops were formed most easily when the disturbance gave a ratio of $l/d = 4.42$. For viscous liquids this ratio is somewhat greater. (See Section VII.)

If it is assumed that the initial disturbances are of uniform magnitude, then a constant time, the disintegration time T , elapses from the beginning of the disturbance to the formation of a drop. Consequently, a definite jet length, the disintegration length L , is developed until a drop is cut off, which length increases in proportion to the velocity. Figure 6a represents the

disintegration of a jet without air influence for an initial disturbance of $l/d = 4.42$. Compare Figure 10a, the picture of a jet of water at a velocity of $v = 3.1$ m/s, the shape of which is not appreciably affected by the air. Since the initial disturbances fluctuate, the disintegration length at constant velocity is not perfectly constant, but oscillates about a mean value. The differences in the disturbances may be so great that the jet is simultaneously broken into drops at several points. The drop formed at the disintegration point continues in the direction of the jet axis, and oscillates about its position of equilibrium. In viscous liquids the damping due to internal friction is so great that these oscillations die out very quickly. (See Figures 12a, 12b, and 13d.)

c) Drop formation with the influence of the air.— In Figure 7 the disintegration length L of a water jet of 0.51 mm diameter is plotted against the velocity v . It is obvious from the figure that, above a certain velocity v , the disintegration length L is no longer proportional to v , but reaches a maximum value and then decreases. This is partially explained by the fact that the disintegration time $T = L/v$ decreases under the influence of the air. The aerodynamic forces act in this case like the wind blowing over water, as shown in Figure 8. Here also the surface of the water is given a definite initial disturbance. The air velocity then increases over the wave crests and decreases over their troughs. At the same time the pressure decreases over the crests and increases over the troughs. The wave motion is thus intensified. In like manner the air acts on the constrictions, so that drops are formed and the disintegration of the jet is accelerated. Figure 6b shows the effect of the aerodynamic forces on the jet, while Figure 10c shows the actual condition of a water jet of 1 mm diameter at $v = 7.8$ m/s.

d) Wave formation due to action of air.— When the velocity is further increased, the initial disturbances become one-sided under the augmented influence of the air. They seem to be trying to bend the jet and develop, under the increased influence of the air, more rapidly than rotationally symmetric disturbances. Figure 6c shows the influence of the aerodynamic forces on the jet corresponding to Figure 8. The surface tension in this case has a retarding effect on the wave formation since it tends to return the jet to its original form with the minimum surface tension. With water and gas oil, due to their small viscosity, the air does not permit the development of a

very pronounced wave form. Separate liquid particles are thrown off and form a cone-shaped mantle about the core of the jet. Figure 11c shows the wave formation with gas oil. The waves show very clearly with the viscous liquids, glycerine and castor oil. (Fig. 12d.) In this case the jet develops into a peculiarly distorted wave line, which is illustrated by Figure 9. For the highest and lowest parts, the air resistance is the smallest, and therefore the jet velocity is the greatest. The variation in velocity along the jet is shown by the v line in Figure 9a. The jet shown in Figure 9b was constructed with the aid of this line. Figure 10c is referred to for comparison.

e) Complete disintegration of the jet.— When the velocity is further increased, the jet loses all regularity of form. The liquid flowing from the nozzle is broken up in a chaotic and entirely irregular manner under the influence of the air. How much this is due to internal vaporization of the liquid and the formation of vortices in the nozzle cannot be determined from the pictures. (Figs. 10g, 11f, and 11g.) The transitions between the different jet forms take place gradually, so that the formation of drops and of waves, or of waves and complete disintegration of the jet, may take place simultaneously.

V. DESCRIPTION OF THE PICTURES

a) Water.— The jet pictures show the characteristic forms for the liquids tested. Figures 10a to 10g refer to water and a nozzle diameter d of 1 mm or 1.04 mm (a to e, glass nozzles; b and g, brass nozzles). Figure 10a shows drop formation without influence of air for $v = 3.1$ m/s. The jet is smooth and clear, and the initial disturbances do not become recognizable until near the end of the jet, where they cause it to break up. The ratio l/d varies between 4.5 and 7. To the naked eye there is a clouding and thickening of the jet at the disintegration point. Consequently, the disintegration length can be measured directly. As the velocity increases, the disintegration length also increases and attains a maximum value. Figure 10b shows this condition, which occurs at $v = 4.7$ m/s, while l/d remains practically unchanged.

With further increase in velocity the disintegration

length suddenly decreases, and the jet sometimes breaks up simultaneously in several places. The value of the disintegration length varies greatly. Figure 10c is for $v = 7.8$ m/s. Shortly after its exit from the nozzle the jet shows rotationally symmetric disturbances with small l/d which, however, cannot cause the jet to break up. The disintegration is caused by disturbances at $l/d = 3.5$ to 4.5. The decrease in the disintegration length and the occurrence of disturbances at smaller l/d is attributable to the increasing influence of the air. Figure 10d shows the drop formation with traces of wave formation at $v = 10$ m/s. The determination of the jet length with the naked eye is impossible when waves are formed, since the jet gradually grows thicker. Its determination by photography depends largely on the judgment of the observer, since the transition from the wavy jet to the disrupted form is gradual and not sharply defined.

Figure 10f shows the beginning of complete disintegration at $v = 34$ m/s, while Figure 10g shows complete disintegration at $v = 40$ m/s. No clear, continuous jet can now be seen, since the air caught up and carried in the jet divides the liquid in an irregular and confused manner.

b) Gas oil.— Figures 11a to 11g refer to gas oil. At low velocities the photographs are quite similar to those of water. Figure 11a shows the drop formation for $d = 0.51$ at $v = 5.1$ m/s, and Figure 11b shows the maximum jet length of 125 mm at $v = 6.6$ m/s. Figure 11c shows the decrease in the jet length and the beginning of the wave formation. Figure 11d shows the waviness quite clearly at $v = 15.6$ m/s. However, several smaller and larger drops are still formed in the jet under the influence of the surface tension and the action of the air. Figure 11e shows the wave formation at $v = 18$ m/s for $d = 1.04$ mm, while Figures 11f and 11g show complete disintegration at $v = 40$ and 73 m/s, respectively. Here complete atomization occurs.*

*The cloudiness in the photographs was caused by gas-oil mist deposited on the glass plate when the needle valve was opened. It was not possible to prevent this precipitation entirely. Neither was it possible to obtain clear photographs without the protection afforded by the glass plate, since the gas-oil mist ruined the silver-bromide film.

c) Glycerine.-- Figures 12a to 12e show the disintegration of a glycerine jet. Figure 12a shows the drop formation from a jet of 1.04 mm diameter at the low velocity of 6.6 m/s. The ratio l/d is considerably higher than for water or gas oil, namely, 7 to 8.5. Hence the drop diameters also increase. It is worth noting that, because of the damping effect of the viscosity of glycerine, the oscillation of the drops about their position of equilibrium, which is noticeable with water and with gas oil, no longer occurs.

The drop formation is unchanged up to very high velocities, while disintegration length increases with the velocity. Figure 12b shows the drop formation from a jet of 0.51 mm diameter at $v = 24$ m/s. This jet attains its maximum length $v =$ about 30 m/s, when wave formation begins. Figure 12c shows this phenomenon at 28 m/s, while Figures 12d and 12e exhibit it at velocities of 38 and 43 m/s, respectively. No formation of mist occurred with glycerine, as in Figure 11g, with gas oil.

d) Castor oil.-- Figures 13a to 13e refer to castor oil and a nozzle diameter of $d = 0.51$ mm. In this case it was no longer possible to obtain a picture of drop formation with a horizontal jet, since the jet sank so rapidly, due to its great disintegration length. On the contrary, the drop-formation length was measured by means of a curved measuring rod. At the same time the size of the drops was determined by catching them in a solution of tannic acid and measuring them under the microscope. From the size of the drops the wave length during their formation was determined.

In order also to show photographically that a pure drop formation occurs with castor oil under the influence of its surface tension, the picture in Figure 13a of a jet falling vertically at a velocity of about 4 m/s, was taken. Here the drop formation is clearly shown. The ratio l/d has increased to a range of about 50 to 70, whereby, of course, the wave length is also increased by the accelerated velocity of the falling jet.

Figures 13b to 13e show the wave formation with castor oil very clearly, the forms being very similar to those for glycerine, only at higher velocities. The deceleration of the part of the liquid cylinder perpendicular to the direction of motion is sometimes so great that loops

are formed in the jet. Figure 13d is practically a continuation of Figure 13e. The wavy jet becomes turbulent and then breaks up into drops.

VI. EFFECT OF JET VELOCITY AND DIAMETER ON DISINTEGRATION LENGTH

In Figures 14 and 15 the disintegration lengths L for water, gas oil, glycerine and castor oil, as determined by means of the measuring stick or from the photographs, are plotted against the velocity v for the nozzle diameter $d = 0.51$ mm.

The L/v curve for water during drop formation is straight at first. Within this range there is consequently a constant disintegration time $T = L/v = 0.0167$ second. Under the influence of the air, the disintegration time decreases, and we obtain a maximum value $L_{\max} = 65$ mm at a velocity $v = 5$ m/s. Then L decreases suddenly, thus causing considerable scattering, and there is a gradual transition into the disintegration length of wave formation.

In the experiments with nozzles of different diameters in drop formation without the influence of air, an increase in disintegration length with nozzle diameter was found. Also the maximum disintegration length increased. The plotting of these curves was omitted because the determination of the disintegration length in drop formation with air influence and with wave formation depends too much on subjective observation and because the experimental values are too much scattered.

Similar results are obtained with the L/v values for gas oil. The maximum disintegration length is greater than for water, due to its greater viscosity. For small velocities, L increases linearly with v the same as for water, but with a disintegration time of $T = 0.017$ second.

With glycerine (fig. 15) the disintegration length is considerably greater than with water and gas oil at the same velocities. Without air influence the disintegration time $T = 0.043$ second. The maximum disintegration lengths are no longer determined by drop formation. In this case

the waviness is already superimposed. The waviness occurs at $v = \text{about } 30 \text{ m/s.}$

The L/v diagram for castor oil does not differ perceptibly in character from the one for glycerine. The distances measured with the curved measuring rod were introduced as the disintegration lengths. In this case the typical increase of L is also manifest. The disintegration time without air influence is $T = 0.26 \text{ second.}$ L_{max} is determined, as in the case of glycerine, not by drop formation, but by the wave formation. It is worth noting that the disintegration point for castor oil recedes more rapidly than for glycerine, which is attributable to the lower specific gravity and the smaller surface tension of castor oil.

The disintegration times T of the liquids tested, as obtained from the disintegration lengths in the region without air influence, are assembled in Table III for different nozzle diameters and are plotted logarithmically in Figure 16 against the nozzle diameter. It is therefore obvious that the disintegration time for all the liquids tested increases with increasing nozzle diameter. We obtained

For water,	$T = L/v = d^{1.5} K,$
" gas oil,	$T = d^{1.5} K',$
" glycerine,	$T = d^{1.2} K'',$
" castor oil,	$T = d^{1.1} K''',$

In these cases K , K' , K'' , and K''' are constants which depend on the physical properties of the liquid and on the size of the initial disturbances. K' is somewhat, K'' and K''' are considerably greater than K .

TABLE III. Disintegration Times for the Liquids Investigated

Nozzle diameter d mm	Disintegration time (sec.) for			
	Water	Gas oil	Glycerine	Castor oil
0.12	0.0018	0.0022	0.008	0.045
0.22	0.0049	0.0052	0.015	0.10
0.31	0.0090	0.010	0.023	0.144
0.51	0.0167	0.017	0.043	0.26
0.71	0.029	0.037	-	0.37
1.04	0.057	0.064	0.111	0.57

VII. DROP FORMATION WITHOUT INFLUENCE OF AIR

In this section the drop formation without influence of air is investigated on the basis of similarity considerations. The determining factors are exclusively inertia, surface tension, and viscosity. The following symbols refer to similar processes in the same or in different liquids:

Index 1 refers to one process, index 2, to a second similar process. Then, for both processes:

l refers to corresponding lengths (cm),
 t " " " times (seconds),
 v " " " velocities (cm/s),
 ρ " " " densities (g./cm³),
 $\eta/\rho = \nu$ " " kinematic viscosities (cm²/s),
 α " " surface tensions (g/cm).

If the forces of inertia and surface tension are exclusively considered, the processes are similar for equal values of the nondimensional indexes:

$$\frac{v_1^2 l_1}{(\alpha/\rho)_1} = \frac{v_2^2 l_2}{(\alpha/\rho)_2} = A \quad (1)$$

or

$$\frac{l_1^3}{t_1^2 (\alpha/\rho)_1} = \frac{l_2^3}{t_2^2 (\alpha/\rho)_2} = \text{const.} \quad (1a)$$

If one compares two processes in a liquid of negligibly small viscosity, these processes are similar according to equation (1a), when

$$\log t = 1.5 \log l + C_1.$$

The curves in Figure 15 for water and gas oil show this slope.

If surface forces and viscous forces are exclusively considered, one obtains similar processes for equal values of the nondimensional indexes

$$\frac{\eta_1 v_1}{\alpha_1} = \frac{\eta_2 v_2}{\alpha_2} = B \quad (2)$$

or

$$\frac{l_1 \eta_1}{t_1 \alpha_1} = \frac{l_2 \eta_2}{t_2 \alpha_2} = \text{const.} \quad (2a)$$

If one compares two processes in a liquid, in which surface tension and viscosity are of outstanding importance, he finds the processes similar, according to equation (2a), when

$$\log t = \log l + C_2.$$

This slope is approximately correct for castor oil.

For processes in which inertia, viscosity, and surface tension must be considered simultaneously, similarity is obtained when equations (1) and (2) are both fulfilled. If the quantities in one process (index 1) are given, we obtain for the quantities in a second process (index 2) from equations (1) and (2):

$$l_2 = l_1 \frac{v_2^2 (\alpha/\rho)_1}{v_1^2 (\alpha/\rho)_2} \quad (3)$$

$$v_2 = v_1 \frac{v_1 (\alpha/\rho)_2}{v_2 (\alpha/\rho)_1} \quad (4)$$

$$t_2 = t_1 \frac{v_2^3 (\alpha/\rho)_1^2}{v_1^3 (\alpha/\rho)_2^2} \quad (5)$$

For one and the same liquid no similar processes can be obtained. When, however, a process in one liquid is given, the dimensions are then clearly established for a similar process in a second liquid. In Table IV a process in water (index 1) is converted by calculation into a similar process in castor oil (index 2). For water a jet diameter of $d_1 = 0.051$ cm and a velocity of $v_1 = 320$ cm/s are assumed. Then, for the process in castor oil

$$d_2 = d_1 \frac{(\alpha/\rho)_1 v_2^2}{(\alpha/\rho)_2 v_1^2} = 0.051 \text{ (cm)} \frac{70.8 \text{ (cm}^3/\text{s}^2) \cdot 8.78^2 \text{ (cm}^2/\text{s)}^2}{34.7 \text{ (cm}^3/\text{s}^2) \cdot 0.01^2 \text{ (cm}^2/\text{s)}^2} =$$

$$= 80000 \text{ cm} = 800 \text{ m,}$$

$$v_2 = v_1 \frac{(\alpha/\rho)_2 v_1}{(\alpha/\rho)_1 v_2} = 320 \text{ (cm/s)} \frac{34.7 \text{ (cm}^3/\text{s}^2) \cdot 0.01 \text{ (cm}^2/\text{s)}}{70.8 \text{ (cm}^3/\text{s}^2) \cdot 8.78 \text{ (cm}^2/\text{s)}} =$$

$$= 0.18 \text{ cm/s} = 1.8 \text{ mm/s.}$$

If one would experimentally establish similar processes for these liquids, he would arrive at practically unattainable dimensions.

Drop-formation phenomena without influence of air may, however, be calculated for a standard liquid. The disintegration times and the jet diameters are so calculated, according to equations (3) and (4), as to yield the time and diameter for a similar process with water. These times and diameters, reduced to water, are extraordinarily small. For example, a castor-oil jet of 0.12 mm diameter corresponds to a water jet of only 7.65×10^{-8} mm diameter. The diameters d and the disintegration times T for water, gas oil, glycerine, and castor oil are compared in Table III, while Table IV gives the values for gas oil, glycerine, and castor oil as converted to a similar process for water.

TABLE IV. Conversion of Nozzle Diameter d and of Disintegration Time T to the Similar Process in Water

d (mm)	T (s)	d_w (mm)	T_w (s)
Gas oil			
0.12	0.0022	0.75×10^{-3}	8.15×10^{-7}
0.22	0.0052	1.38×10^{-3}	1.93×10^{-6}
0.31	0.010	1.94×10^{-3}	3.71×10^{-6}
0.51	0.017	3.20×10^{-3}	6.3×10^{-6}
0.71	0.037	4.43×10^{-3}	13.7×10^{-6}
1.04	0.064	6.50×10^{-3}	23.7×10^{-6}
Glycerine			
0.12	0.008	1.64×10^{-5}	1.08×10^{-8}
0.22	0.015	3.00×10^{-5}	2.03×10^{-8}
0.31	0.023	4.25×10^{-5}	3.11×10^{-8}
0.51	0.043	7.00×10^{-5}	5.81×10^{-8}
0.71	-	-	-
1.04	0.111	1.43×10^{-4}	15.0×10^{-8}
Castor oil			
0.12	0.045	7.68×10^{-8}	1.82×10^{-11}
0.22	0.10	1.40×10^{-7}	3.57×10^{-11}
0.31	0.144	1.99×10^{-7}	5.16×10^{-11}
0.51	0.26	3.26×10^{-7}	9.30×10^{-11}
0.71	0.37	4.55×10^{-7}	1.34×10^{-10}
1.04	0.57	6.67×10^{-7}	2.03×10^{-10}

If T is plotted logarithmically over d (fig. 17), the values lie on a curve whose slope is 1:1 for small values of d and 1:1.5 for large values of d .

For similar initial disturbances we have, according to Weber (reference 3),

$$T = K \left[\left(\frac{\rho}{9 \eta^2} \alpha d \right)^{1.5} + \left(\frac{\rho}{9 \eta^2} \alpha d \right) \right] \quad (6)$$

This function is introduced in Figure 17 for comparison, in which the constant K is so chosen that the best possible agreement is obtained.

In Figure 18 the ratio l/d is plotted against d for the conditions of disintegration. In this case the values determined from the photographs or from the drop diameters are plotted against the logarithm of the diameter converted to water. (Table V.)

TABLE V. Ratio of Wave Length l to Jet Diameter d
(Index f refers to the liquid tested; index w , to the conversion to water)

Liquid	d_f (mm)	d_w (mm)	l/d	Determined by
Water	0.51	0.51	4.3 to 7	Photography
Gas oil	0.51	3.25×10^{-3}	4.5 " 6	"
Glycerine	0.51	7.12×10^{-5}	6 " 14	"
Castor oil	0.31	1.99×10^{-7}	30 " 40	Drop size

For l/d according to Weber (loc. cit.), we have

$$\frac{l}{d} = \pi \sqrt{2} \sqrt{1 + \frac{3 \eta}{\sqrt{\rho \alpha d}}} \quad (7)$$

This function is introduced into Figure 18. The measured points follow a similar course.

VIII. SUMMARY

The purpose of the investigation was to obtain information regarding the disintegration phenomena in liquid jets of various densities, viscosities and surface tensions for different jet diameters and velocities. The liquids tested were water, gas oil, glycerine and castor oil.

Simple apparatus is described for the production of a jet of 0.1 to 1.0 mm in diameter with velocities ranging from 2 to 70 m/s. The observation of the jet was accomplished through shadow pictures, which were obtained by means of electric sparks. These pictures show four characteristic forms: drop formation without air influence, drop formation with air influence, formation of

waves, and complete disintegration of the jet. In the case of drop formation without air influence, there is a disintegration time which is independent of the velocity. This is different for different jet diameters and liquids. The actual relationship between the disintegration time and the jet diameter can be determined on the basis of similarity relations.

REFERENCES

1. Triebnigg, H.: The Injection Process in Compressorless Diesel Engines. Der Einblase- und Einspritzvorgang bei Dieselmotoren, Vienna, 1925.

Wöltjen, A.: Ueber die Feinheit der Brennstoffzerstäubung, Dissertation, Darmstadt, 1925.

Kuehn, R.: Motorwagen, Vol. 31, 1928, p. 325.

Riehm, W.: V.D.I. Zeitschrift, Vol. 68, 1924, p. 641.
2. Rayleigh, Lord: On the Instability of Jets. Proceedings of the London Mathematical Society, Vol. 10, 1878.
3. Weber, C.: Zum Zerfall eines Flüssigkeitsstrahles. Z. f. angew. Math. u. Mech., Vol. 11, No. 3, 1931.
In this work the theory of Lord Rayleigh is extended to viscous liquids, and the influence of the air on drop formation and on wave formation is investigated.

Translation by

R. A. Castleman, jr.,
Bureau of Standards,

and

Dwight M. Miner,
National Advisory Committee
for Aeronautics.

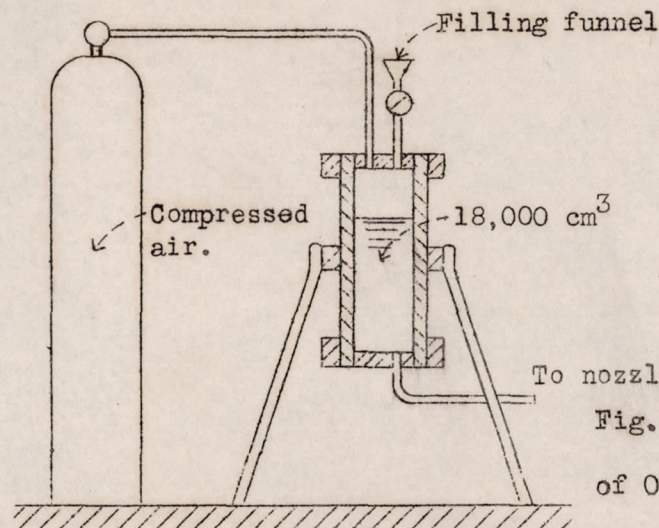


Fig. 2 Arrangement for nozzles of 0.7 to 2 mm dia.

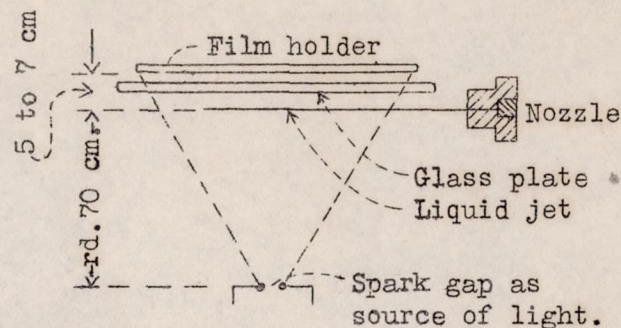


Fig. 3 Arrangement for taking shadow pictures by means of electric sparks.

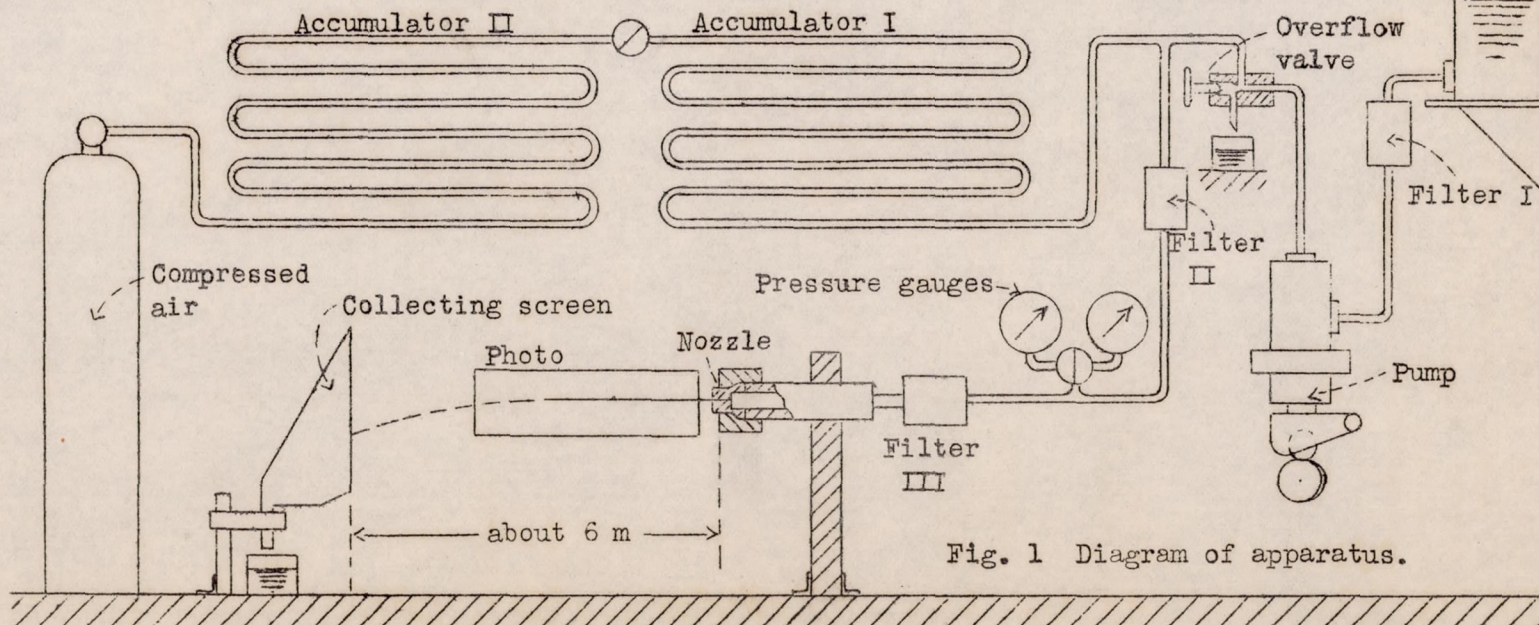


Fig. 1 Diagram of apparatus.

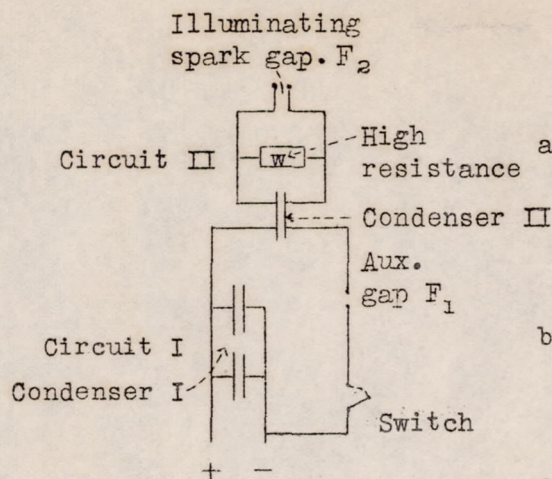


Fig. 4 Wiring system for obtaining the illuminating sparks.

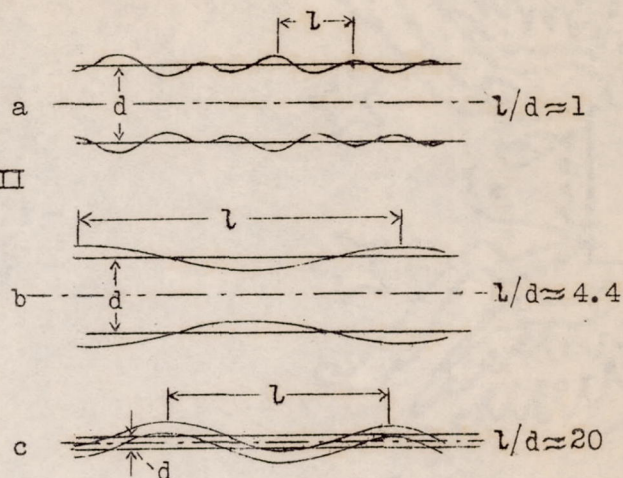


Fig. 5 Surface disturbances (a and b, rotationally symmetric; c, one-sided wavelike)

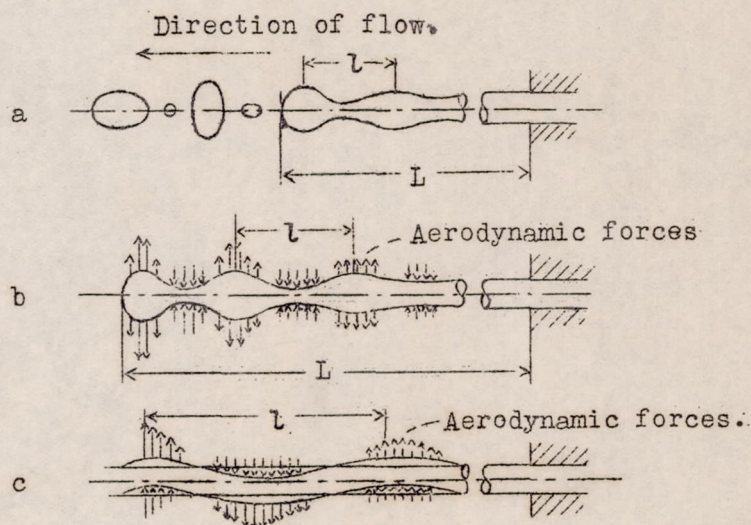


Fig. 6 Disintegration phenomena (a, drop formation without air influence; b, drop formation with air influence; c, wave formation through air influence.)

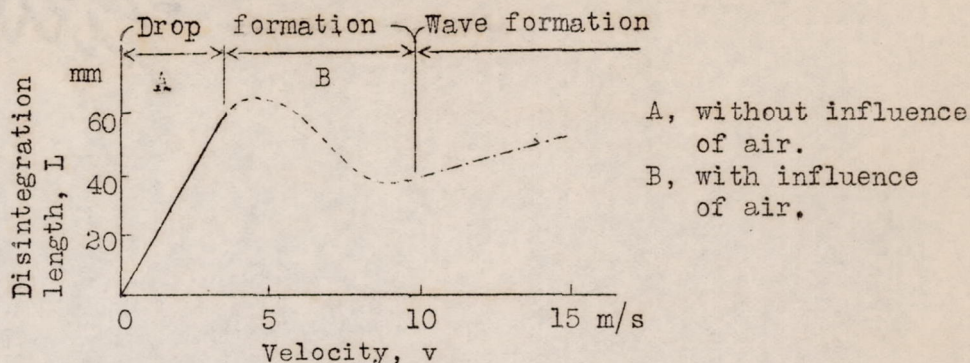


Fig. 7 Disintegration length L of a water jet of 0.51 mm diameter plotted against velocity v .

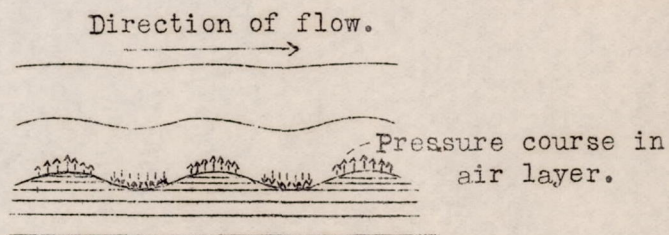


Fig. 8 Effect of moving air on a water surface.

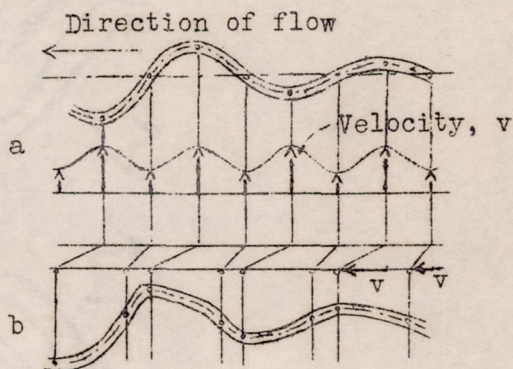


Fig. 9 Formation of distorted wave line.

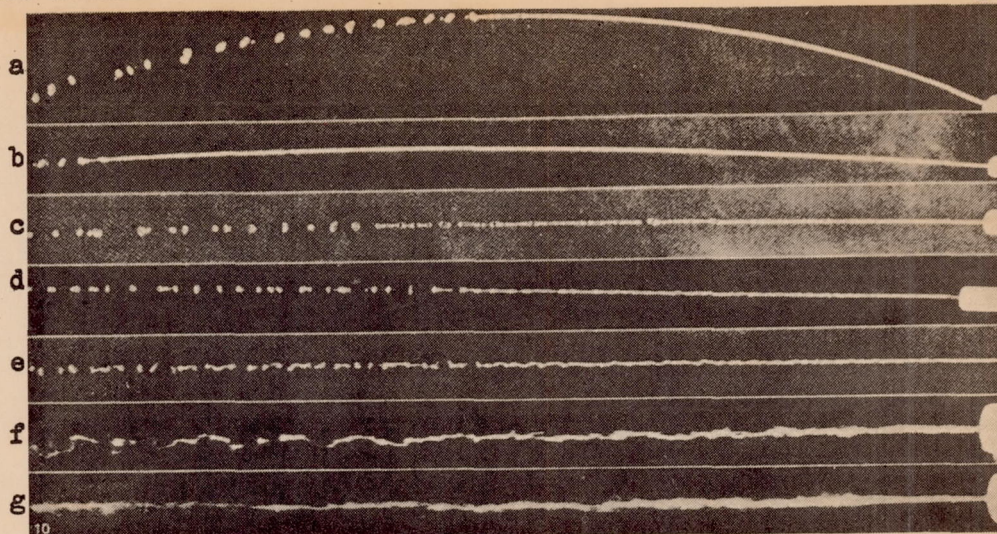


Fig. 10 Water jet.

- (a) Glass nozzle, $d = 1$ mm, $v = 3.1$ m/s, drop formation without air.
 (b) " " , $d = "$ " , $v = 4.7$ " , max.drop-formation length.
 (c) " " , $d = "$ " , $v = 7.8$ " , drop formation with air.
 (d) " " , $d = "$ " , $v = 10.0$ " , drop form.with incipient waves.
 (e) " " , $d = "$ " , $v = 24.0$ " , wave formation.
 (f) Brass " , $d = 1.04$ " , $v = 34.0$ " , beginning of disintegration.
 (g) " " , $d = "$ " , $v = 40.0$ " , complete disintegration.

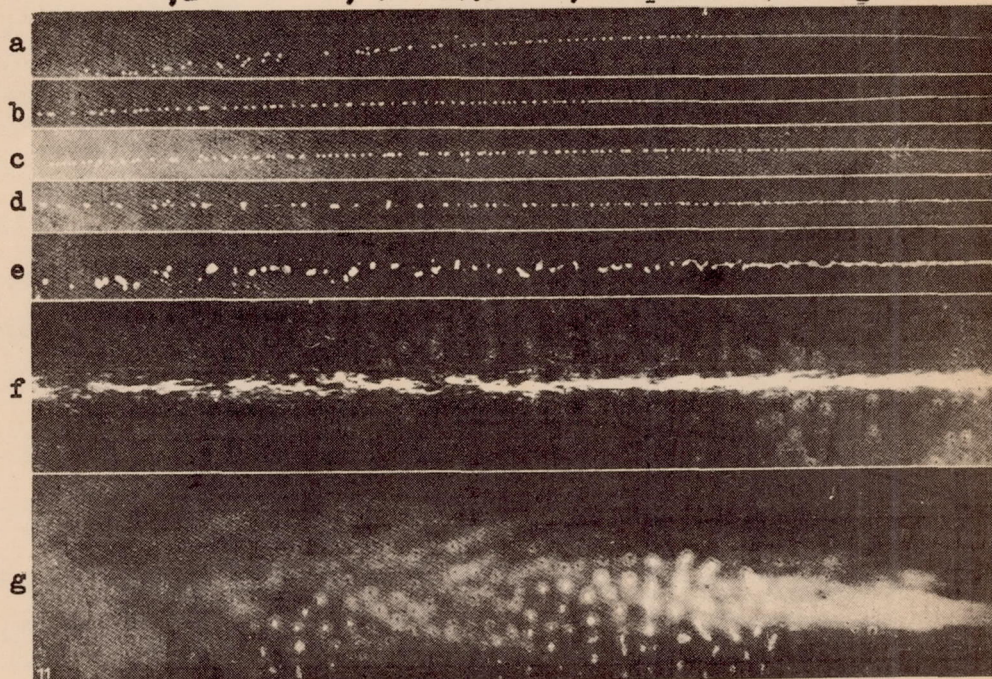


Fig. 11 Gas-oil jet.

- (a) Brass nozzle, $d = 0.51$ mm, $v = 5.1$ m/s, drop formation without air.
 (b) " " , $d = "$ " , $v = 6.6$ " , max.drop-formation length.
 (c) " " , $d = "$ " , $v = 7.5$ " , drop formation with waviness.
 (d) " " , $d = "$ " , $v = 15.6$ " , wave formation.
 (e) " " , $d = 1.04$ " , $v = 18.0$ " , wave formation.
 (f) " " , $d = "$ " , $v = 40.0$ " , complete disintegration.
 (g) " " , $d = "$ " , $v = 73.0$ " , complete disintegration.

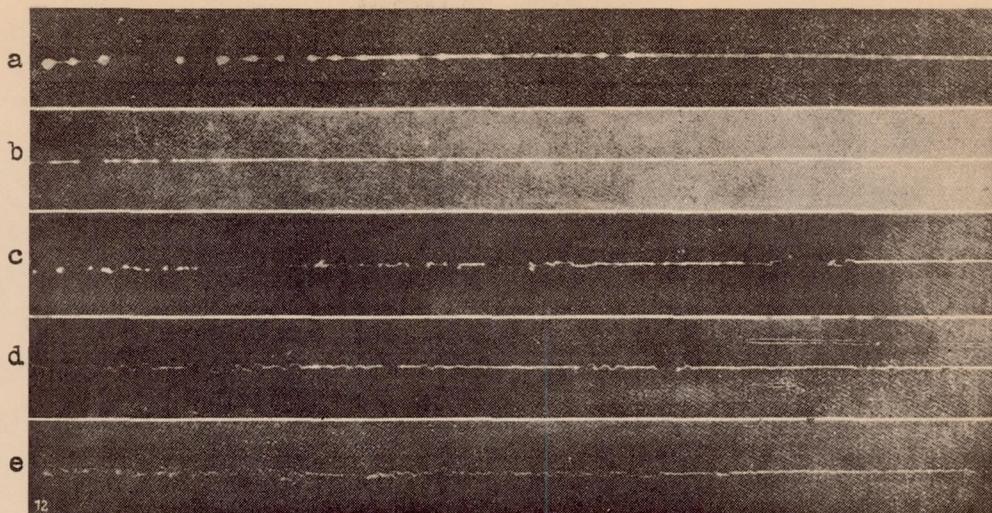


Fig. 12 Glycerine jet (a = distance of right-hand edge of picture from nozzle).

- (a) Brass nozzle, $d = 1.04$ mm, $v = 6.6$ m/s, $a = 90$ cm, drop formation.
 (b) " " , $d = 0.52$ " , $v = 24.0$ " , $a = 51$ " , drop formation.
 (c) " " , $d =$ " " , $v = 28.0$ " , $a = 105$ " , drop form, with incipient waves.
 (d) " " , $d =$ " " , $v = 38.0$ " , $a = 68$ " , wave formation.
 (e) " " , $d =$ " " , $v = 43.0$ " , $a = 100$ " , wave formation.

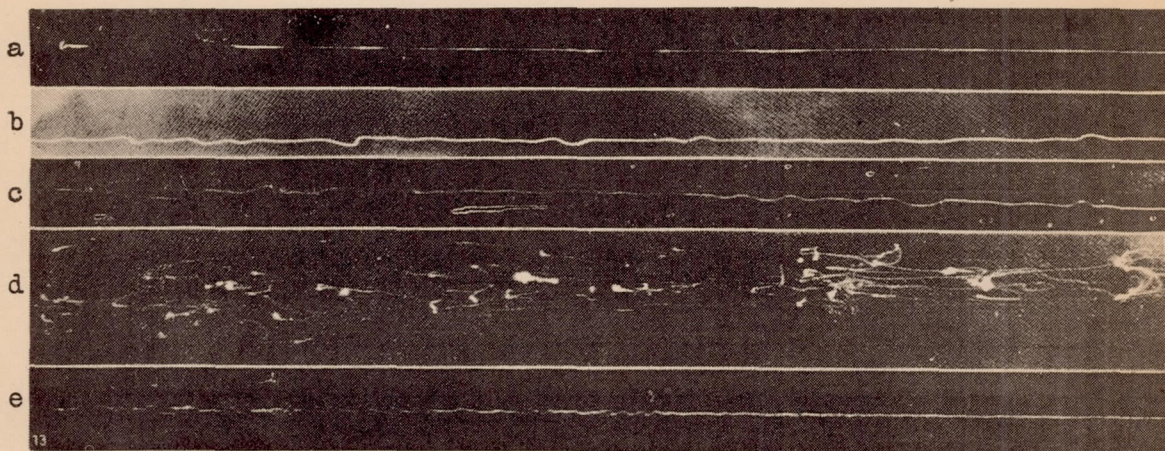


Fig. 13 Castor oil jet (a = distance of right-hand edge of picture from nozzle).

- (a) Brass nozzle, $d = 0.51$ mm, $v \approx 4$ m/s, drop formation, falling jet.
 (b) " " , $d =$ " " , $v = 18$ " , $a = 128$ cm, wave formation.
 (c) " " , $d =$ " " , $v = 40$ " , $a = 19$ " , wave formation.
 (d) " " , $d =$ " " , $v = 45$ " , $a = 70$ " , wave formation.
 (e) " " , $d =$ " " , $v = 73$ " , $a = 7$ " , wave formation.

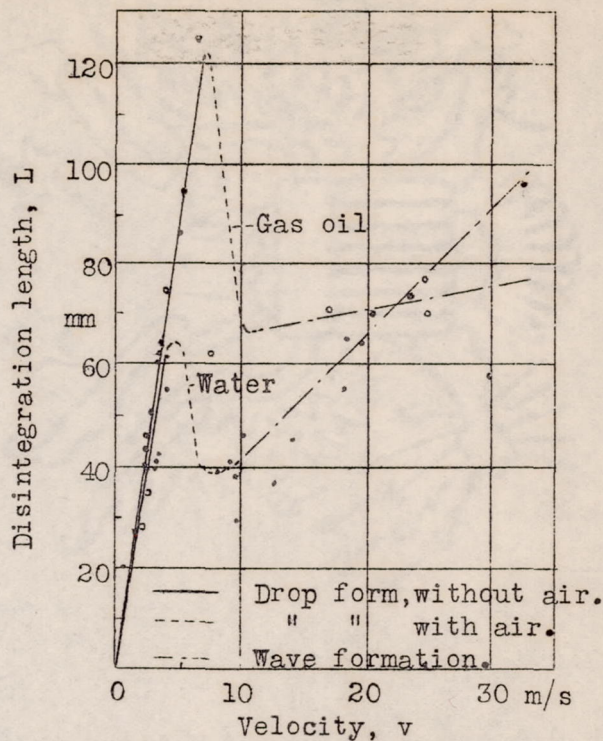


Fig. 14 Disintegration length L plotted against jet velocity v at 0.51 mm nozzle diameter for water and gas oil.

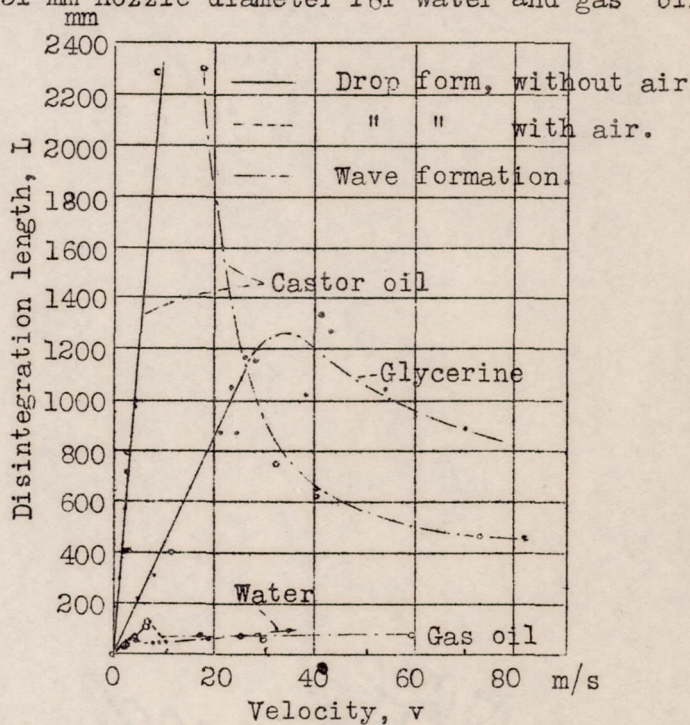


Fig. 15 Disintegration length L plotted against jet velocity v at 0.51 mm nozzle diameter for glycerine and castor oil.

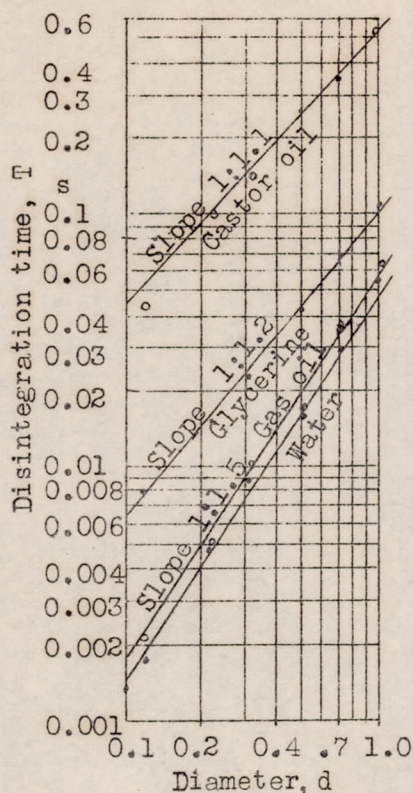


Fig. 16 Disintegration time T plotted against jet diameter d in logarithmic coordinates according to Table III

The following equations refer to Figs. 17, 18.

$$T = K \left[\left(\frac{\rho \alpha}{9\eta^2} d \right)^{3/2} + \frac{\rho \alpha}{9\eta^2} d \right] *$$

$$\frac{l}{d} = \pi \sqrt{2} \sqrt{1 + \frac{3\eta}{\rho \alpha d}} *$$

* (according to C. Weber)

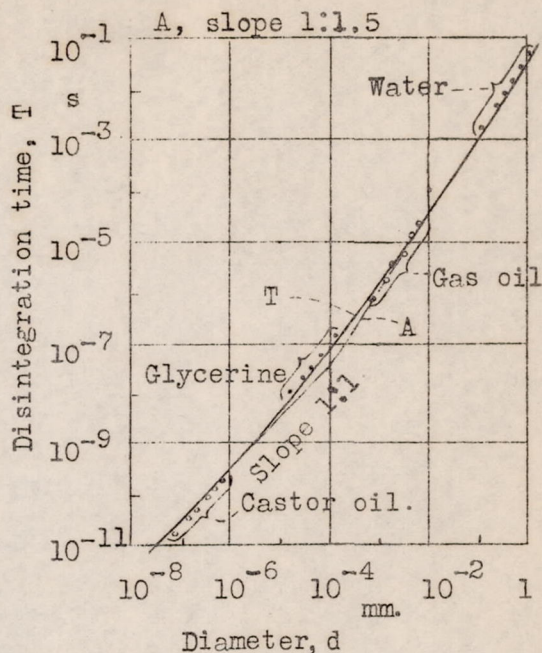


Fig. 17 Drop-formation time T (without air influence) plotted against jet diameter d (referred to water as standard liquid) in log. coordinates according to Table IV

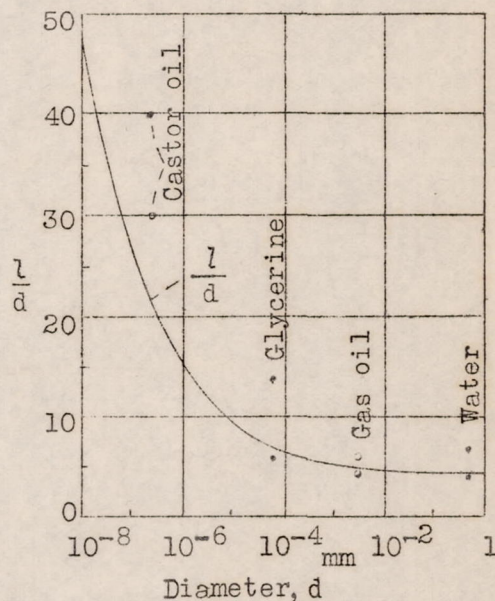


Fig. 18 Ratio of wave length to jet diameter (l/d) (without air influence) plotted against diameter d according to Table V (d in log. scale)